# Concerted expression of a cell cycle regulator and a metabolic enzyme from a bicistronic transcript in plants

Laura Lorenzo-Orts, Janika Witthoeft, Jules Deforges, Jacobo Martinez, Sylvain Loubery, Aleksandra Placzek, Yves Poirier, Ludwig Hothorn, Yvon Jaillais, Michael Hothorn

# Concerted expression of a cell-cycle regulator and a metabolic enzyme from a bicistronic transcript in plants

Laura Lorenzo-Orts[1], Janika Witthoeft[2], Jules Deforges[3], Jacobo Martinez[1,2], Sylvain Loubéry[4], Aleksandra Placzek[2,+], Yves Poirier[3], Ludwig A. Hothorn[5,#], Yvon Jaillais[6], Michael Hothorn[1,2]

[1]Structural Plant Biology Laboratory, Department of Botany and Plant Biology, University of Geneva, Geneva, Switzerland.

[2]Friedrich Miescher Laboratory of the Max Planck Society, Tübingen, Germany

[3]Department of Plant Molecular Biology, University of Lausanne, Lausanne, Switzerland

[4]Department of Botany and Plant Biology, University of Geneva, Geneva, Switzerland.

[5]Institute of Biostatistics, Leibniz University, Hannover, Germany.

[6]Laboratoire Reproduction et Développement des Plantes, Université de Lyon, ENS de Lyon, UCB Lyon 1, CNRS, INRA, F-69342 Lyon, France.

[+]Present address: Max Planck Institute for Biology of Ageing, Cologne, Germany.

[#]retired

correspondence: michael.hothorn@unige.ch

## Abstract

**Eukaryotic mRNAs frequently contain upstream open reading frames (uORFs), encoding small peptides which may control translation of the main ORF (mORF) by various mechanisms. Here we report the identification of a bicistronic transcript in Arabidopsis, in which the uORF encodes an ortholog of the cell cycle regulator CDC26 whose genome locus was previously unknown. AtCDC26 is part of the plant anaphase**

**promoting complex / cyclosome (APC/C), regulates accumulation of APC/C target proteins and controls cell division, growth and embryo development. AtCDC26 is translated together with the inorganic polyphosphatase AtTTM3 from a single transcript conserved in the plant lineage. While there is no apparent biochemical or physiological connection between the two gene products, concerted AtCDC26 and AtTTM3 transcription and translation occurs in different plant tissues and organs. Our work reveals that uORFs in plants may code for functional proteins not involved in the translational regulation of the mORF.**

## Introduction

uORFs are coding sequences in the 5' untranslated region (UTR) of mRNAs. Many uORFs code for small, non-conserved peptides[1,2] and regulate expression of the mORF[3]. While a significant fraction of fungal, animal and plant genes contain uORFs[4], only few functional uORF-derived peptides have been found in cells and tissues[1,5]. In plants, several uORFs have been genetically characterized in transcription factors, metabolic enzymes, membrane transporters and signaling proteins[6]. uORFs regulate the expression of the mORF during growth and development[7], in response to stress[8,9] or to changes in nutrient availability[10]. As in other eukaryotes, plant uORFs are involved in translational repression of the mORF[7] and in the nonsense mediated decay (NMD) of the respective mRNA[11–13].

A fraction of uORFs do not encode small peptides but rather independent, functional proteins, which are transcribed together with the mORF from *bona fide* bicistronic transcripts[14]. Eukaryotic transcripts encoding for more than one protein have been initially reported from vertebrates, where the transforming growth factor-beta family ligand GDF1 is transcribed together with ceramide synthase 1 from a single 3 kb transcript[15]. Other examples

include the p16INK4a gene, which contains two overlapping open reading frames coding for distinct proteins involved in cell cycle regulation[16]. A similar gene architecture has been reported for the mammalian XLαs/Gαs gene. Here, the two translation products code for the extra-large G-protein XLαs and for a sequence-unrelated protein ALEX, which directly binds XLαs[17]. A uORF located in the mammalian A2A adenosine G-protein coupled receptor gene encodes the ~ 15 kDa uORF5 protein, whose expression is regulated by A2A activation[18]. These examples may suggest that mORF and uORF protein products are often functionally and/or biochemically linked[14], but mORF/uORF pairs with no apparent biological connection have been described as well[19].

**Results**

Here we report a novel uORF with unusual properties located in the annotated 5' UTR of *TTM3* in Arabidopsis. *AtTTM3* encodes an inorganic polyphosphatase that releases inorganic phosphate from short-chain linear polyphosphates, a storage form of phosphate in many pro- and eukaryotes[20,21]. *TTM3* is a conserved single copy gene in Arabidopsis and many other plant species (Extended Data Fig. 1a). To define physiological functions for TTM3, we analyzed different *ttm3* mutant alleles: *ttm3-1* maps to the *TTM3* ORF (Fig. 1a), completely abolishes TTM3 expression and protein accumulation (Fig. 1b) and reduces hypocotyl and root growth, in agreement with an earlier report[20] (Fig. 1d, e). A second T-DNA insertion in the 5' UTR of *TTM3* (*ttm3-2*) likely causes a knock-out of TTM3, impairs embryo development and blocks seed germination (Fig. 1c, 3d). *ttm3-4* maps to the 3' UTR, shows reduced TTM3 transcript and protein levels (Fig. 1b) and consistently, a weak growth phenotype (Fig. 1d,e). The observed inconsistencies between the *ttm3-1* and *ttm3-2* mutant lines prompted us to generate an additional CRISPR/Cas9-based mutant. The resulting *ttm3-3* allele harbors a 16 base-pair deletion in the *TTM3* coding sequence (Extended Data Fig. 1b)

that abolishes TTM3 protein accumulation and also reduces *TTM3* transcript levels *in planta* (Fig. 1b). To our surprise, *ttm3-3* mutants did neither resemble the root and hypocotyl growth phenotypes of *ttm3-1* plants nor the *ttm3-2* embryo phenotype (Fig. 1d, e).

We investigated these phenotypic differences by complementing *ttm3-1* and *ttm3-2* mutant alleles with the fluorescent protein-tagged TTM3-mCITRINE expressed under the control of the *TTM3* promoter, including the annotated 5' UTR. Even though TTM3-mCITRINE protein levels were low compared to endogenous TTM3, we observed full complementation of the different *ttm3* alleles, suggesting that the observed phenotypes were specific to the *TTM3* locus (Fig. 2a, b). We next analyzed TTM3-mCITRINE and TTM3-GUS transgenic reporter lines and found that TTM3 is a cytoplasmic/nuclear localized protein expressed in ovules, roots and hypocotyls, in good agreement with the observed phenotypes (Extended Data Fig. 2a, b). We next complemented the embryo phenotype of *ttm3-2* plants with versions of TTM3 compromised in either substrate binding or catalysis[21] (Fig. 2c). To our surprise, catalytically inactive versions of TTM3 could fully complement the *ttm3-2* mutant phenotype (Fig. 2d, e), indicating that the enzymatic activity of TTM3 is dispensable for proper embryo development.

Close inspection of the *TTM3* locus revealed the presence of a putative uORF in the annotated 5'UTR of TTM3, ending 8 base-pairs upstream of the mORF start codon (Fig. 3a, Extended Fig. 3a). The uORF encodes a putative peptide of 65 amino acids, sharing significant sequence homology with CDC26 superfamily proteins (Fig. 3a). CDC26, whose genome locus was previously unknown[22,23], forms a component of the APC/C, an E3-ubiquitin ligase that targets substrates for degradation, allowing for cell cycle progression[24]. AtCDC26 protein accumulates in different plant tissues throughout development (Fig. 3b). Since *ttm3* phenotypes did not seem to be related to TTM3 protein levels or its catalytic

activity, we analyzed AtCDC26 transcript and protein expression levels in *ttm3-1*, *ttm3-3* and *ttm3-4* mutants. Although transcript levels were lower, we found no observable differences for AtCDC26 protein levels in the non-lethal *ttm3-1, ttm3-3* and *ttm3-4* mutants (Fig. 3c).

Based on these observation, we hypothesized that complementation of our *ttm3-1* and *ttm3-2* mutant lines (Fig. 2a-d) may have been due to the re-introduction of functional AtCDC26, present in what we thought would be the *TTM3* 5' UTR. We could indeed detect wild-type levels of AtCDC26 in our *ttm3-2* complemented lines (Fig. 2f). Ubiquitous expression of the AtCDC26 CDS alone fully rescued *ttm3-2* embryo lethality and *ttm3-1* defective root and hypocotyl growth (Fig. 3d-f), suggesting that the observed and reported[20] phenotypes for *ttm3-1* were caused by interference with *CDC26* expression, rather than *TTM3* loss-of-function.

We next tested if AtCDC26 is a *bona fide* component of the Arabidopsis APC/C. We performed immunoprecipitation assays followed by mass-spectrometry in wild-type plants expressing epitope-tagged AtCDC26-6xHA. AtCDC26 interactors included APC1, APC5, APC6 and APC7/CDC27B, which have been previously shown to interact with CDC26 in human[25], and in addition APC2 and APC8, together forming the APC/C complex (Fig. 2g)[24,26]. The plant APC/C regulates cell division and affects many aspects of plant growth and development[22,27]. To test whether *ttm3-1* mutant plants have abnormal cell divisions cycles, we quantified GFP levels in *ttm3-1* plants expressing fluorescent tagged Cyclin B1;1 (CYCB1;1-GFP[28]). CYCB1;1 is a marker of cell division and a target of the APC/C[29,30]. We found that CYCB1;1-GFP expression and protein levels (inferred from the GFP fluorescent signal) are less variable and overall reduced in *ttm3-1* plants vs. wild-type plants, indicating that the mutant is defective in cell division and CYCB1;1-GFP protein stability, respectively (Fig. 3h). Together, our findings suggest that AtCDC26 is plant cell-cycle regulator and part

of the Arabidopsis APC/C. Importantly, we did not recover TTM3 peptides in our immunoprecipitation assays and recombinant AtTTM3 and AtCDC26 showed no detectable interaction in *in vitro* isothermal titration calorimetry assays, suggesting that TTM3 does not form part of the plant APC/C complex (Extended Data Fig. 4).

*CDC26* and *TTM3* are both present in the entire plant lineage and their ORFs are always in close proximity (Fig. 4a, Extended Data Fig. 3a). The *CDC26* stop codon may be spaced ~150 base-pairs apart from the start codon of *TTM3* (e.g. in *Chlamydomonas reinhardtii* and *Marchantia polymorpha*), be separated by only a short sequence (in Arabidopsis), or the ORFs may even overlap, as found for example in tomato and maize (Fig. 4a, Extended Data Fig. 3a-c). As *CDC26* and *TTM3* are always in close proximity, we speculated that both proteins could be expressed from a single bicistronic transcript. We performed northern blots with probes against *CDC26* and *TTM3* in wild-type and *ttm3-1* mutant plants. We detected a major transcript of ~1,200 nucleotides using both probes, which is absent in *ttm3-1* plants (Fig. 4b). Next, we performed 5' and 3' RACE experiments with CDC26 specific primers and recovered a transcript of similar size (Fig. 4c). Sequencing of 5' RACE products confirmed the presence of the *CDC26* and *TTM3* ORFs in a single transcript in wild-type plants (see Supplementary Information). One additional, minor transcript was recovered in the RACE experiments, encoding CDC26 only (see Supplementary Information). The presence of both transcripts could be confirmed in RT-PCR experiments (Fig. 4d). cDNA clones suggest that *CDC26* and *TTM3* are encoded in a single transcript in Chlamydomonas, tomato and maize (Extended Data Fig. 3b). To test if AtCDC26 and AtTTM3 are translated from a single mRNA, we performed *in vitro* translation assays in wheat germ extracts where products were labeled with $^{35}$S methionine. Two protein products migrating at the expected size of AtCDC26 and AtTTM3, respectively, were produced from an *in vitro* transcribed

144 *CDC26-TTM3* transcript (Fig. 4e). Mutating the start codon of either *CDC26* or *TTM3*
145 eliminated translation of the respective gene product, but did not affect translation of the
146 other ORF (Fig. 4e). Together our *in vivo* and *in vitro* experiments reveal that CDC26 and
147 TTM3 are transcribed and translated from a single transcript, yielding two proteins with
148 different biochemical and physiological functions. The *ttm3-3* allele and the complementation
149 experiments using catalytically inactive versions of TTM3 together suggest that neither the
150 enzyme itself nor its catalytic function impact the phenotypes described for the *TTM3* locus[20].
151 Our loss-of-function phenotypes reveal an essential role for CDC26 in Arabidopis, as
152 previously seen in animals[31]. The fact that CDC26 is expressed from a conserved uORF in
153 the *TTM3* gene suggests that this bicistronic transcript may have important regulatory
154 functions in plant cell cycle control. Translation of different cyclin-dependent kinases from a
155 single transcript occurs via cell-cycle regulated internal ribosome entry sites (IRES) in
156 metazoa[32], but it is unknown if this mechanism is present in plants[6]. Notably, expression of
157 AtCDC26 from a strong ubiquitous promoter alone can rescue all observed phenotypes, while
158 expression of AtCDC26 under control of its native promoter requires the endogenous 3'UTR
159 or the presence of the *TTM3* mORF (Extended Data Fig. 5a-e). Complementation of a ttm3-2
160 mutant with a construct harboring a mutated CDC26 start codon (*CDC26-TTM3) did not
161 rescue the ttm3-2 embryo lethal phenotype. (Fig. 5a,b). In contrast, we observed stunted-
162 growth and 'broom-head' phenotypes previously seen in *APC6* and *APC10* knock-down
163 mutants[33] or in a *APC8* missense allele[34], when complementing *ttm3-2* plants with a construct
164 harboring a mutated *TTM3* start codon (CDC26-*TTM3) (Fig. 5a,c). *CDC26* transcript levels
165 are high in plants expressing CDC26-*TTM3 but protein levels were reduced compared to
166 wild-type, indicating that CDC26 and TTM3 may require to be translated in a concerted
167 fashion (Fig. 5d). To investigate this issue further, we performed polysome profiling

experiments. We find the *TTM3* transcript associated with polysomes in wild-type seedlings, but to a lesser extend in CDC26-*TTM3 plants, indicating that TTM3 translation recruits the biscistronic transcript to polysomes (Fig. 5e).

It has been previously reported that the Target of rapamycin (TOR) complex can regulate uORF translation and loading of the respective transcripts to polysomes[10,35]. We thus tested whether CDC26 and TTM3 expression is regulated by TOR. As previously reported, the uORF-containing transcript *bZIP11* is shifted to monosomes upon treatment with the TOR-inhibitor AZD8055 (AZD), while the polysome profile of *TTM3* seems unaffected (Fig. 5f). In line with this, TTM3 and CDC26 protein levels are not significantly reduced in seedling treated with the TOR-inhibitors KU63794 and AZD, when compared to the actin loading control (Fig. 5g). These experiments together indicate that TOR may not have a major role in the translational regulation of CDC26 and TTM3.

Finally, we tested if the *CDC26-TTM3* transcript is regulated by NMD, as previously reported for other uORF containing transcripts in Arabidopsis[11–13]. We found *CDC26-TTM3* transcript levels to be higher in wild-type plants treated with cycloheximide (CHX), an inhibitor of protein translation that represses NMD[36] (Fig. 6a), or in known NMD mutant backgrounds (Fig. 6b). Consistently, also CDC26 and TTM3 protein levels were increased in NMD mutants (Fig. 6c). Together, these experiments indicate that the *CDC26-TTM3* bicistronic transcript is regulated by nonsense-mediated decay.

## Discussion

In Arabidopsis, uORF-containing mRNAs represent more than 30% of the transcriptome and these uORFs may control translation efficiency and mRNA stability of the mORF[6]. Here we present a novel uORF in Arabidopsis not involved in the regulation of translation, but rather

forming an essential component of the plant APC/C complex. This CDC26 subunit shows a monocistronic gene architecture in other eukaryotes, but is encoded in a biscistronic transcript upstream of the inorganic polyphosphatase TTM3 in the entire green lineage from algae to higher land plants (Extended Data Fig. 3a). Our finding now provides the genome locus for AtCDC26, whose transcript had been previously detected [22,23]. Our genetic analyses suggest no strong functional connection between AtCDC26 (which our analyses define as an essential gene) and AtTTM3 (whose enzymatic function appears to be dispensable at least in the growth conditions tested, compare Fig. 2), and AtTTM3 does not seem to interact biochemically with stand-alone CDC26 or the plant APC/C (Fig. 3g, Extended Data Fig. 4). It is however of note that inorganic polyphosphates promote cell cycle exit in bacteria[37] and fungi[38], and we thus cannot exclude a functional connection between TTM3 and CDC26.

We did not observe regulation of the *TTM3* mORF by the *CDC26* uORF, but rather we found that translation of the mORF recruited the bicistronic transcript to polysomes, enhancing CDC26 translation, and thus protein levels *in planta*. While the mechanism of concerted CDC26 and TTM3 translation remains to be investigated, we found that in some species both ORFs are located at a very short distance, or even overlap (Extended Data Fig. 3). This makes TTM3 translation by ribosome re-initiation unlikely[39]. We confirmed that transcripts featuring an overlapping arrangement of *CDC26* and *TTM3* ORFs are translated in wheat germ extracts, leading to full-length CDC26 and TTM3 protein products (Extended Data Fig. 6). In addition, we could not detect an internal ribosome entry site (IRES) in the *CDC26* coding sequence, and a synthetic *CDC26-TTM3* transcript with altered codons did still support translation of both proteins (Extended Data Fig. 6). We thus speculate that leaky ribosome scanning may reach the *TTM3* start codon[40], as it has been previously suggested for viral bicistronic transcripts translated in plants[41]. In line with this, we do not observe major

changes in CDC26 and TTM3 expression upon treatment with TOR inhibitors, with TOR affecting ribosome re-initiation in plants[10,35]. We could however confirm that the *CDC26-TTM3* transcript is under regulation by nonsense-mediated decay (Fig. 6). As the Arabidopsis NMD pathway counteracts cyclin-dependent kinases activity required for cell cycle progression[42,43], NMD of the *CDC26-TTM3* transcript could represent an additional regulatory mechanism of CDC26 function in the control of plant cell cycle.

Taken together, we demonstrate that a novel cell cycle regulator in plants is expressed from a conserved uORF in a gene coding for a metabolic enzyme. Our genetic and biochemical characterization of the *CDC26 TTM3* locus now enables the mechanistic dissection of bicistronic transcription and translation in plants.

## METHODS

**Plant material and growth conditions.** *ttm3-1* (SALK_133625), *ttm3-2* (FLAG_368E06), and *ttm3-4* (SALK_050319) T-DNA insertion lines were obtained from NASC (Nottingham Arabidopsis Stock Center). The *ttm3-3* mutant was generated using CRISPR/Cas9. Specifically, the *TTM3*-specific sequence 5'-ATTGAGACGGAGATGAGCAGCGG-3' (*sgTTM3*) was cloned into the PTTK352 vector[44], containing Cas9 in a cassette with hygromicin-resistance and RFP as selection-markers. *Arabidopsis* Col-0 plants were transformed with pTTK352-sg*TTM3* (see *generation of transgenic lines*). T1 generation plants were selected via hygromicin resistance. *ttm3-3* was identified by PCR followed by sequencing. In T2 generation, seeds not expressing RFP (lacking Cas9) were selected. Plants were grown under conditions of 50 % humidity, 22 °C and 16 h of light.

**Real-time quantitative reverse transcription polymerase chain reaction** RNA was extracted with the Rneasy Plant Mini Kit (Qiagen). 2 µg of RNA was treated with Dnase I (Qiagen), copied to cDNA using an Oligo dT and the SuperScript™ II Reverse Transcriptase (Invitrogen). Transcript levels were estimate using the SYBR Green PCR Master Mix (Applied Biosystems), and transcript abundance was normalized to *ACT8*. Values indicate the mean ± standard deviation of three replicates. Primer sequences can be found in Extended Data Table 1.

**Protein expression and generation of antibodies** TTM3 was produced and purified as described[45]. For generation of the TTM3 antibody, rabbits were immunized with purified TTM3 dialyzed against phosphate-buffered saline (PBS). The resulting serum was affinity-

purified over AtTTM3-coupled Affigel 15 (Biorad, www.bio-rad.com), eluted in 200 mM glycine pH 2.3, 150 mM NaCl and stored in PBS pH 7.5.

CDC26 was cloned into pMH-TrxT vector, providing an N-terminal 6xHis-StrepII-Thioredoxin tag (HST) and a tobacco etch virus (TEV) protease cleavage site. CDC26 expression was induced in *Escherichia coli* BL21 (DE3) RIL cells with 0.25 mM isopropyl β-D-galactoside (IPTG) at $OD_{600}$ ~0.6, and grown at 16 °C for 16 h. Cells were collected by centrifugation (4,500 g, 30 min), resuspended in lysis buffer (20 mM Tris pH 8, 500 mM NaCl, 1 mM $MgCl_2$, 5 mM β-mercaptoethanol and cOmplete™ EDTA-free Protease Inhibitor Cocktail (Merck) and homogenized (Emulsiflex C-3, Avestin). HST-CDC26 was isolated from the lysate via tandem $Ni^{2+}$ and StrepII affinity purification (HisTrap HP 5 ml, GE Healthcare; Strep-Tactin Superflow high capacity, IBA), and purified further by size-exclusion chromatography (Superdex 75 HR10/30, GE Heathcare). The HST-CDC26 fusion protein was incubated with TEV protease (1:100 molar ratio) for 16 h at 4 °C. CDC26 was recovered by a second $Ni^{2+}$ affinity step followed by size exclusion chromatography. The molecular weight of the purified protein was determined to be 7.3 kDa (as predicted) by MALDI-TOF mass spectometry. A polyclonal CDC26 antibody was generated in rabbit (Eurogentec) and purified as described for AtTTM3.

**Western blotting** Plant material was snap-frozen in liquid nitrogen and homogenized with mortar and pestle. The material was resuspended in 50 mM Tris pH 8.0, 150 mM NaCl, 0.5 % Triton X-100 and cOmplete™ EDTA-free Protease Inhibitor Cocktail (Merck). 20-50 µg of total protein extract (estimated by Bradford, Bio-Rad), pre-boiled for 5 min, was run on a 10 % SDS-PAGE gel. Proteins were blotted onto nitrocellulose membranes (GE Healthcare), then blocked using TBS buffer containing 0.1 % (v/v) tween 20, 5 % (w/v) powder milk.

Membranes were incubated for 1 h at room temperature with CDC26 or TTM3 antibodies, and then with an anti-rabbit peroxidase conjugate (1 μg $\mu l^{-1}$) antibody (Calbiochem), or with an anti-HA-HRP (Miltenyi Biotec) (dilution 1:5,000). Membranes were then stained with Ponceau (0.1 % (w/v) Ponceau S in 5 % (v/v) acetic acid). Bands corresponding to RuBisCO (~56 kDa) are shown as a loading control.

**Phenotyping assays** For root length measurements, stratified seeds (2-5 d, 4 °C, in darkness) were germinated on ½ MS medium, containing ½ MS (Duchefa), 0.5 g/L MES, 0.8 % (w/v) agar, 1 % (w/v) sucrose, pH 5.7. After 4 days, seedlings were transferred to new plates and grown for 7 d at 22 °C, 16 h of light. For hypocotyl length measurements, seeds were plated in ½ MS and exposed 3 h to light after 2-5 d of stratification (4 °C, in darkness). Seedlings were grown for 6 d in darkness at 22 °C. Measurements were done using the NeuronJ plugin[46] in Fiji[47]. The simultaneous comparisons of root and hypocotyl growth against wild type for a fold change was performed for a Dunnett-type procedure ratio-to-control[48] assuming approximate normal distributed variance heterogeneous errors using the package 'mratios' in R-CRAN. Adjusted two-sided p-values are reported in figure legends.

For germination assays, seeds were plated in ½ MS and stratified for 2-5 d at 4 °C in darkness. Germination rates were determined after 2 d of light exposure. Imaging of *ttm3-2* embryos was performed by opening siliques from *ttm3-2* heterozygous plants. Seeds were mounted on a cover slip and covered by a destaining solution containing 2.7 g/L chloral hydrate, 0.25 % (v/v) glycerol. Samples were destained for 16 h at 4 °C and imaged under a conventional light microscope.

**Generation of transgenic lines** For constructs cloned in pH7m34GW (pH7) and pB7m34GW (pB7)[49] vectors (compare Extended Data Table 1), promoters were cloned first into the pDONR P4-P1R vector, coding sequences into pDONR221 or pDONR207 vectors, and C-terminal tags into pDONR P2R-P3 vector with the Gateway™ BP Clonase™ II Enzyme mix (Merck). Constructs were assembled by the Gateway™ LR Clonase™ Enzyme mix (Merck). If avoidance of gateway cloning sites was necessary, , constructs were cloned into the pGreenII vector (pGIIB) (GenBank reference: EF590266.1) or in a modified-version, pGIIH by Gibson assembly[50]. In the pGIIH vector, the gene conferring resistance to Basta was replaced by a hygromycine resistance gene cassette by Gibson [50]. *Agrobacterium tumefaciens*, strain pGV2260, was transformed with pH7, pB7,or with the binary vectors pGIIH or pGIIB (pSOUP was used as a help plasmid, GenBank reference: EU048870.1). *Arabidopsis thaliana* was transformed using the floral dip method[51]. T1 plants were selected using hygromycin (pH7, pGIIH) or Basta (pB7, pGIIB), and homozygous plants were analyzed in T3 generation.

**β-glucuronidase (GUS) reporter assay** Plants or plant organs were fixed in 2 % (v/v) formaldehyde, 50 mM sodium phosphate buffer pH 7.0 for 30 min at room temperature. After two washes with 50 mM sodium phosphate buffer, plants were submerged into a staining solution containing 0.5 mM potassium ferrocyanide, 0.5 mM potassium ferricyanide and 0.1 mM X-GlcA. Vacuum was applied 3 times, 1 min per pulse. Staining occurred for 2 h at 37 °C. After washing samples twice (1 h incubation per wash) with 96 % (v/v) ethanol and 60 % (v/v) ethanol, respectively, plants were stored in 20 % (v/v) ethanol. Pictures were taken with a Canon EOS 1000D SLR digital camera coupled to a stereomicroscope Zeiss SteREO Discovery.V8.

**Isothermal titration calorimetry (ITC)**. CDC26 and TTM3 interaction was assayed using a Nano ITC (TA Instruments) at 25 °C. Both proteins were gel-filtrated into ITC buffer (20 mM Tris pH 8, 500 mM NaCl, 1 mM $MgCl_2$). 10 µL of CDC26 (at 200 µM) was injected into 250 µM TTM3 protein, in 25 injections at 150 s intervals. Data was corrected for the dilution heat and analyzed using the software NanoAnalyze (version 3.5) provided by the manufacturer.

**Immunoprecipitation followed by LS-MS** Ws-4 wild-type and Ubi10p:CDC26-6xHA seedlings were snap-frozen in liquid nitrogen, homogenized with mortar and pestle and resuspended in protein extraction buffer (PBS buffer pH 7.4, 1 mM EDTA, cOmplete™ EDTA-free Protease Inhibitor Cocktail from Merck) and including 0.1 % (v/v) Triton X-100. The lysate was incubated with anti-HA microbeads (µMACS HA Isolation Kit, Miltenyi Biotec) at 4 °C for 2 h. Beads were washed 4 times with protein extraction buffer supplemented with 0.05 % (v/v) Triton X-100, 1 time with protein extraction buffer, and eluted with the denaturing elution buffer provided in the kit. The elution was boiled for 5 min at 95 °C and separated into a 10 % SDS-PAGE gel. Silver staining was performed as previously described[52]. Bands present in the Ubi10p:CDC26-6xHA sample and absent or reduced in the Ws-4 sample were cut and analyzed by LC-MS at the Proteomics Core Facility (Centre Medical Universitaire, CMU, Geneva). Results were analyzed using the software Scaffold (Proteome Software Inc, Portland, Oregon), setting a threshold of 99.9 % for peptide and protein identification.

**RNA extraction and northern blot** Col-0 wild-type and *ttm3-1* mutant seedlings were snap-frozen in liquid nitrogen and homogenized with mortar and pestle. RNA was isolated using

TRIZOL (Gibco BRL, Grand Island, NY, USA) according to the supplier's instructions. 5 µg of total RNA was treated with DnaseI (Qiagen) and recovered with the standard phenol-chloroform purification[53] (UltraPure™ Phenol:Chloroform:Isoamyl Alcohol (25:24:1, v/v), Merk). Samples containing 7 µg of RNA, 0.1 % (v/v) formaldehyde and 1x MOPS buffer (20 mM MOPS pH 7.0, 5 mM NaOAc, 1 mM EDTA) were heated for 15 min at 60 °C, and loaded into a formaldehyde gel (1 % (w/v) agarose, 1x MOPS, 1 % (v/v) formaldehyde). Electrophoresis was performed for 3 h at 60 V in MOPS buffer. The gel was blotted overnight in a hybond-N membrane (GE Healthcare) in 10x SSC buffer (150 mM sodium citrate, 1.5 M NaCl). The membrane was cross-linked by UV and pre-hybridized with church buffer (0.25 M PBS pH 7.2, 1 mM EDTA. 1 % (w/v) BSA and 7 % (w/v SDS) for 45 min at 65 °C. 50 ng of *CDC26* and *TTM3* probes (compare Extended Table 2), labeled with dCTP[α-$^{32}$P] (PerkinElmer), were hybridized overnight at 65 °C. Membranes were washed with 1x SSC buffer supplemented with 0.1 % SDS, and subsequently exposed to a X-ray film for 3 d at -80 °C.

**5' and 3' Rapid amplification of cDNA ends (RACE)** 3' RACE was performed using the Thermofisher 3' RACE kit following the manufacturer's instructions. For the 5'RACE, RNA was copied to cDNA using RACE_SP1 primer (compare Extended Data Table 2). A polyA tail was added artificially with a terminal transferase (NEB) using ATP as substrate. The cDNA was used as a template in a second PCR with an oligo dT fused to an adaptor primer (AP) and RACE_SP2 primer. A third PCR with RACE_SP3 and AUAP gave a 5' RACE specific product. The major band was cut and sent for sequencing with TTM3_3'_F and CDC26_RT_F primers (compare Extended Data Table 2). Alternatively, RACE products were cloned in pCR™8 (Merck) and sequenced with M13 forward and T7 forward primers.

***In vitro* transcription and translation** *CDC26-TTM3* transcript (including the *CDC26* start codon and 1268 down-stream base-pairs) was cloned into pCR™8 (Merck), under the control of the T7 promoter. Mutations were performed by site-directed mutagenesis (see Extended Data Table 2). Capped RNA was transcribed *in vitro* using the MEGAscript™ T7 Transcription Kit (Merck). 1 µg of RNA was added to wheat germ extract (Promega), and *in vitro* translation was performed as recommended by the manufacturer. Products from the *in vitro* translation, labeled with $^{35}$S methionine, were loaded onto a 12 % polyacrylamide gel and run for ~ 2 h at 100 V. The gel was washed with water and exposed to a X-ray film for 4 h at -80 °C.

**Confocal microscopy** CYCB1;1-GFP seeds were crossed with the *ttm3-1* mutant allele. Selection of CYCB1;1 insertion was done via Basta selection, and the presence of the *ttm3-1* insertion was confirmed by genotyping. Plants were analyzed in F3 generation. 4 d old seedlings were fixed in PBS with 4 % (v/v) paraformaldehyde and 0.01 % (v/v) Triton X-100 for 1 h at room temperature after vacuum infiltration. Samples were washed twice in PBS and incubated for one week in the dark at room temperature in ClearSee solution[54]. Next, samples were mounted between slide and coverslip in ClearSee solution and imaged under an SP8 confocal microscope (Leica) equipped with a 10x NA 0.3 lens and a HyD detector using 488 nm excitation and 492-533 nm emission, a pinhole of 1AU and a pixel size of 180 nm. Number of GFP-expressing cells was quantified[55] using the software Fiji[47]. The transmission image was used to estimate cell length; the last cortical cell, the length of which was approximately 1.5 times its width, was defined as the last cortical meristematic cell and was used to define the limit of the meristem. Maximal intensity projections of the confocal z

393 stacks were performed and the look-up table “Fire” was used to optimize the visualization of
394 GFP signal. Localization of the TTM3-mCITRINE fusion protein was analyzed in 5 d old
395 seedlings again using the SP8 confocal microscope.
396
397 **Polysome profiling**. Wild-type and two independent transgenic lines expressing CDC26-
398 *TTM3 (in *ttm3-2* background) were grown for 10 days in ½ MS medium. Alternatively, 7-
399 days old wild-type seedlings were treated for 4 h in 1/8 MS liquid medium containing either 1
400 µM AZD or DMSO (mock). Seedlings were snap-frozen and homogenized with mortar and
401 pestle. The material was resuspended in 1 volume of polysome extraction buffer, containing
402 200 mM Tris pH 9.0, 200 mM KCl, 1 % DOC, 1 % PTE, 35 mM $MgCl_2$, 1 mM DTT and 100
403 µg/mL cycloheximide. After 15 min incubation on ice, the cell extract was centrifuged for 15
404 min at 16000 g, 4 °C. The clarified extract was loaded on top of a 15 % to 60 % sucrose
405 gradient. Polysomal fractions were separated by ultracentrifugation on a SW55 rotor
406 (Beckman), at 50000 rpm, 1 h 15 min, 4 °C, and collected from top to bottom into 10
407 fractions using a gradient holder (Brandel) coupled to a spectrophotometer. RNA from each
408 fraction was extracted using TRIZOL (Gibco BRL, Grand Island, NY, USA), according to
409 the supplier's instructions. After a second RNA precipitation (500 mM ammonium acetate,
410 2.5 volumes of ethanol, 1 h, -20 °C), RNA was reverse transcribed into to cDNA using the
411 M-M-MLV RNAse H minus kit (Promega) and oligo dT, and analyzed by qRT-PCR as
412 described before. The fraction 1 was excluded from the analysis since it contained very low
413 amount of both *TTM3* and *ACT* mRNAs. The percentage of TTM3 mRNA in each fraction
414 (relative to *ACT2*) was determined as described[56].
415

**Data availability** Authors confirm that all relevant data has been included in this paper and it is available upon reasonable request.

## FIGURE LEGENDS

**Figure 1 | Different *ttm3* mutant alleles show inconsistent phenotypes related to embryo development and plant growth. a**, Overview of *ttm3* alleles in the *TTM3* locus. **b**, *TTM3* transcript and protein levels in *ttm3* mutants relative to wild-type, estimated by qPCR (left) and western blot (right), respectively (error bars represent standard deviation (SD) of three replicates). **c**, Developing wild-type and *ttm3-2* embryos in different stages (scale bars are 20 μm). Quantification of embryo-developmental phenotypes in seeds from *ttm3-2* heterozygous plants is shown alongside. **d**, Seedling root growth assay (n=13 seedlings per genotype). Representative *ttm3* mutant and wild-type seedlings are shown. Quantification of root length (normalized to wild-type root length average) is represented with box plots (p-values: *ttm3-1*/wild-type<0.001, *ttm3-3*/WT=0.693, *ttm3-4*/WT=0.019). **e**, Hypocotyl growth assay (n=62 seedlings per genotype). Representative seedlings are shown. Hypocotyl length measurements (normalized to hypocotyl length average in wild-type) are represented with dots (p-values: *ttm3-1*/WT<0.001, *ttm3-3*/WT=<0.001, *ttm3-4*/WT=0.002).

**Figure 2 | Catalytically inactive TTM3 variants complement *ttm3* phenotypes when expressed from the native promoter including the 5' UTR. a**, Complementation of the embryo lethal *ttm3-2* allele with TTM3-mCITRINE restores seed germination. Shown are representative seedlings with the corresponding germination rates (%). Total number of seeds analyzed is shown in brackets. Scale bars correspond to 0.5 cm. **b**, Seedling root growth assay with *ttm3-1* plants expressing TTM3-mCITRINE (n=12). Representative seedlings are shown. Quantification of root length (normalized to wild-type) is represented in box plots

(p_values: #8/WT=0.479, #12/WT=0.600). **c,** Ribbon diagram of the AtTTM3 tunnel domain (in yellow) with a triphosphate molecule bound in the center, coordinated by a $Mn^{2+}$ ion (pink sphere). Arg52 involved in substrate binding[21] is shown in cyan, three glutamate residues required for metal co-factor binding and catalysis[21] are highlighted in magenta (Glu2, Glu4 and Glu169). **d**, AtTTM3 mutant proteins, impaired in either substrate binding or catalysis fully complement the *ttm3-2* mutant phenotype when expressed from the *TTM3* promoter including the annotated 5' UTR, as judged from seed germination assays. Shown are germination rates, with total number of seeds analyzed in brackets. **e**, TTM3-mCITRINE is expressed at lower levels than endogenous TTM3, as judged from western blotting, while **f,** CDC26, translated from the *TTM3* 5'UTR, is expressed at wild-type levels.

**Figure 3 | A uORF in *TTM3* encodes the cell-cycle regulator AtCDC26. a**, Arabidopsis *CDC26* maps to the 5' UTR of *TTM3* and contains the N-terminal CDC26 motif required for APC/C binding. Sequence identity is shown alongside **b**, CDC26 and TTM3 proteins are expressed in different tissues and stages of development. **c**, *CDC26* transcript and protein levels in different *ttm3* mutants relative to wild-type, measured by qPCR (left) and western blot (right), respectively (error bars represent SD, n=3). **d**, Germination assay in *ttm3-2* plants complemented with Ubi10p:CDC26-6xHA. Shown are percentages of germinated seeds in total number of seeds (in brackets, scale bars are 0.5 cm). AtCDC26-6xHA protein levels were detected by western blot using an anti-HA antibody (right). **e**, Seedling root growth assay in *ttm3-1* plants complemented with Ubi10p:CDC26-6xHA vs. *ttm3-1* and normalized to wild-type (n=24) (p-values: #8/WT=0.920, #6/WT=0.017). **f,** Hypocotyl growth assays in *ttm3-1* plants complemented with Ubi10p:CDC26-6xHA in relation to wild-type (n=53) (p-values: #6/WT=0.037, #8/WT=0.447). **g**, APC/C components recovered by IP-MS (arrows

464 indicate bands present in CDC26-6xHA and absent or reduced in wild-type protein extracts).
465 AtCDC26 protein interactors are highlighted in the human APC/C structure (PDB-ID 4ui9[24])
466 (bottom). **h**, Root tips of *ttm3-1* plants (n=6) expressing p:CYCB1;1-GFP show less GFP
467 expressing-cells and an overall lower GFP intensity compared to wild-type plants expressing
468 CYCB1;GFP. Quantification of GFP signal is shown alongside. Scale bars correspond to 25
469 μm.
470
471 **Figure 4 | CDC26 is expressed from a bicistronic transcript in plants. a**, Phylogenetic tree
472 of *CDC26* and *TTM3* ORFs from different plant species. Distances between the *CDC26*
473 termination codon and the *TTM3* start codon are indicated in base-pairs. **b**, Northern blotting
474 reveals a major transcript detected with *CDC26* and *TTM3* probes and absent in *ttm3-1* plants
475 (indicated with an arrow). **c**, RACE experiments result in cDNA products containing either
476 *CDC26* and *TTM3* ORFs or *CDC26* alone (see Supplementary Information).. *ttm3-1* mutants
477 harbor a truncated transcript containing only the CDC26 uORF (see Supplementary
478 Information). **d**, RT-PCR using primers binding to *CDC26* and *TTM3* confirm the presence
479 of a single *CDC26-TTM3* transcript (blue), absent in *ttm3-1*, and a CDC26 transcript (red),
480 present in low levels in *ttm3-1*. **e**, *In vitro*-translation of an *in vitro* transcribed *CDC26-TTM3*
481 bicistronic transcript results in two proteins of the expected molecular weight. Calculated
482 molecular weight is 7,225 Da and 24,162 Da for AtCDC26 and AtTTM3, respectively.
483 Mutation of the *CDC26* or *TTM3* start codon blocks translation of the respective protein.
484
485 **Figure 5 | TTM3 translation recruits the transcript to polysomes in a TOR-independent**
486 **manner. a**, Transcripts containing mutations in *CDC26* and *TTM3* start codons (*CDC26 and
487 *TTM3, respectively) used for complementation of *ttm3-2* plants. **b**, *CDC26 does not

488 complement *ttm3-2* embryo-lethality, as shown in 4 independent transgenic lines. **c**, *TTM3
489 plants show a phenotype reminiscent of *apc* loss-of-function mutants. Bottom picture shows a
490 detail of wild-type and *TTM3 siliques (scale bar is 2 cm). **d**, CDC26 protein levels are
491 reduced in *TTM3 plants (top), while transcript levels are higher than wild-type (bottom).
492 Error bars denote SD for n=3. **e**, Polysome profile (top) reveals that *TTM3* transcript
493 associates with polysomes in wild-type but not in *TTM3 plants (bottom). Error bars denote
494 SD for n=3. **f**, Polysome profiles of wild-type seedlings treated for 4 h with the TOR-
495 inhibitor AZD8055 (AZD) show changes for *bZIP11*, but not for *TTM3*. Error bars denote SD
496 for n=3. **g**, 4-days old seedlings treated for 3 days with 3 μM TOR-inhibitors show a
497 reduction in CDC26 and TTM3 protein levels comparable to actin (top). *TTM3* mRNA levels
498 are equal or higher upon treatment (bottom).
499
500 **Figure 6 | The CDC26-TTM3 transcript is a target of NMD. a,** Treatment of 5-days old
501 wild-type plants with 20 μM cycloheximide (CHX) for 8 h leads to the accumulation of
502 *SMG7*, a known NMD target, and *CDC26-TTM3* transcript. **b,** *CDC26-TTM3* transcript and
503 protein levels are higher in Arabidopsis *lba1* and *upf3-1* mutants, defective in NMD. Error
504 bars denote SD for n=3.
505
506 **References**


1. Oyama, M. *et al.* Analysis of small human proteins reveals the translation of upstream open reading frames of mRNAs. *Genome Res.* **14,** 2048–2052 (2004).
2. Johnstone, T. G., Bazzini, A. A. & Giraldez, A. J. Upstream ORFs are prevalent translational repressors in vertebrates. *EMBO J.* **35,** 706–723 (2016).

3. Wethmar, K. The regulatory potential of upstream open reading frames in eukaryotic gene expression. *Wiley Interdiscip. Rev. RNA* **5,** 765–778 (2014).
4. Wethmar, K., Barbosa-Silva, A., Andrade-Navarro, M. A. & Leutz, A. uORFdb--a comprehensive literature database on eukaryotic uORF biology. *Nucleic Acids Res.* **42,** D60-67 (2014).
5. Menschaert, G. *et al.* Deep proteome coverage based on ribosome profiling aids mass spectrometry-based protein and peptide discovery and provides evidence of alternative translation products and near-cognate translation initiation events. *Mol. Cell. Proteomics* **12,** 1780–1790 (2013).
6. von Arnim, A. G., Jia, Q. & Vaughn, J. N. Regulation of plant translation by upstream open reading frames. *Plant Sci.* **214,** 1–12 (2014).
7. Zhou, F., Roy, B., Dunlap, J. R., Enganti, R. & von Arnim, A. G. Translational Control of Arabidopsis Meristem Stability and Organogenesis by the Eukaryotic Translation Factor eIF3h. *PLoS ONE* **9,** (2014).
8. Pajerowska-Mukhtar, K. M. *et al.* The HSF-like Transcription Factor TBF1 Is a Major Molecular Switch for Plant Growth-to-Defense Transition. *Curr. Biol.* **22,** 103–112 (2012).
9. Starck, S. R. *et al.* Translation from the 5' untranslated region shapes the integrated stress response. *Science* **351,** aad3867 (2016).
10. Schepetilnikov, M. *et al.* TOR and S6K1 promote translation reinitiation of uORF-containing mRNAs via phosphorylation of eIF3h. *EMBO J.* **32,** 1087–1102 (2013).
11. Kurihara, Y. *et al.* Genome-wide suppression of aberrant mRNA-like noncoding RNAs by NMD in Arabidopsis. *Proc. Natl. Acad. Sci. U. S. A.* **106,** 2453–2458 (2009).
12. Nyikó, T., Sonkoly, B., Mérai, Z., Benkovics, A. H. & Silhavy, D. Plant upstream ORFs can trigger nonsense-mediated mRNA decay in a size-dependent manner. *Plant Mol. Biol.* **71,** 367–378 (2009).

13. Malabat, C., Feuerbach, F., Ma, L., Saveanu, C. & Jacquier, A. Quality control of transcription start site selection by nonsense-mediated-mRNA decay. *eLife* **4,** (2015).

14. Mouilleron, H., Delcourt, V. & Roucou, X. Death of a dogma: eukaryotic mRNAs can code for more than one protein. *Nucleic Acids Res.* **44,** 14–23 (2016).

15. Lee, S. J. Expression of growth/differentiation factor 1 in the nervous system: conservation of a bicistronic structure. *Proc. Natl. Acad. Sci. U. S. A.* **88,** 4250–4254 (1991).

16. Ouelle, D. E., Zindy, F., Ashmun, R. A. & Sherr, C. J. Alternative reading frames of the INK4a tumor suppressor gene encode two unrelated proteins capable of inducing cell cycle arrest. *Cell* **83,** 993–1000 (1995).

17. Klemke, M., Kehlenbach, R. H. & Huttner, W. B. Two overlapping reading frames in a single exon encode interacting proteins—a novel way of gene usage. *EMBO J.* **20,** 3849–3860 (2001).

18. Lee, C., Lai, H.-L., Lee, Y.-C., Chien, C.-L. & Chern, Y. The A2A Adenosine Receptor Is a Dual Coding Gene. *J. Biol. Chem.* **289,** 1257–1270 (2014).

19. Autio, K. J. *et al.* An ancient genetic link between vertebrate mitochondrial fatty acid synthesis and RNA processing. *FASEB J. Off. Publ. Fed. Am. Soc. Exp. Biol.* **22,** 569–578 (2008).

20. Moeder, W. *et al.* Crystal structure and biochemical analyses reveal that the Arabidopsis triphosphate tunnel metalloenzyme AtTTM3 is a tripolyphosphatase involved in root development. *Plant J.* **76,** 615–626 (2013).

21. Martinez, J., Truffault, V. & Hothorn, M. Structural Determinants for Substrate Binding and Catalysis in Triphosphate Tunnel Metalloenzymes. *J. Biol. Chem.* **290,** 23348–23360 (2015).

22. Capron, A., Okrész, L. & Genschik, P. First glance at the plant APC/C, a highly conserved ubiquitin-protein ligase. *Trends Plant Sci.* **8,** 83–89 (2003).

23. Lima, M. de F. *et al.* Genomic evolution and complexity of the Anaphase-promoting Complex (APC) in land plants. *BMC Plant Biol.* **10,** 254 (2010).

24. Chang, L., Zhang, Z., Yang, J., McLaughlin, S. H. & Barford, D. Atomic structure of the APC/C and its mechanism of protein ubiquitination. *Nature* **522,** 450–454 (2015).

25. Hutchins, J. R. A. *et al.* Systematic analysis of human protein complexes identifies chromosome segregation proteins. *Science* **328,** 593–599 (2010).

26. Zachariae, W., Shin, T. H., Galova, M., Obermaier, B. & Nasmyth, K. Identification of subunits of the anaphase-promoting complex of Saccharomyces cerevisiae. *Science* **274,** 1201–1204 (1996).

27. Genschik, P., Marrocco, K., Bach, L., Noir, S. & Criqui, M.-C. Selective protein degradation: a rheostat to modulate cell-cycle phase transitions. *J. Exp. Bot.* **65,** 2603–2615 (2014).

28. Ubeda-Tomás, S. *et al.* Gibberellin Signaling in the Endodermis Controls Arabidopsis Root Meristem Size. *Curr. Biol.* **19,** 1194–1199 (2009).

29. Genschik, P., Criqui, M. C., Parmentier, Y., Derevier, A. & Fleck, J. Cell cycle - dependent proteolysis in plants. Identification Of the destruction box pathway and metaphase arrest produced by the proteasome inhibitor MG132. *Plant Cell* **10,** 2063–2076 (1998).

30. Criqui, M. C. *et al.* Cell cycle-dependent proteolysis and ectopic overexpression of cyclin B1 in tobacco BY2 cells. *Plant J.* **24,** 763–773 (2000).

31. Dickinson, M. E. *et al.* High-throughput discovery of novel developmental phenotypes. *Nature* **537,** 508–514 (2016).

32. Cornelis, S. *et al.* Identification and characterization of a novel cell cycle-regulated internal ribosome entry site. *Mol. Cell* **5,** 597–605 (2000).

33. Marrocco, K., Thomann, A., Parmentier, Y., Genschik, P. & Criqui, M. C. The APC/C E3 ligase remains active in most post-mitotic Arabidopsis cells and is required for proper vasculature development and organization. *Development* **136,** 1475–85 (2009).

34. Zheng, B., Chen, X. & McCormick, S. The Anaphase-Promoting Complex Is a Dual Integrator That Regulates Both MicroRNA-Mediated Transcriptional Regulation of Cyclin B1 and Degradation of Cyclin B1 during Arabidopsis Male Gametophyte Development. *Plant Cell* **23,** 1033–1046 (2011).

35. Schepetilnikov, M. & Ryabova, L. A. Recent Discoveries on the Role of TOR (Target of Rapamycin) Signaling in Translation in Plants. *Plant Physiol.* **176,** 1095–1105 (2018).

36. Rayson, S. *et al.* A role for nonsense-mediated mRNA decay in plants: pathogen responses are induced in Arabidopsis thaliana NMD mutants. *PloS One* **7,** e31917 (2012).

37. Racki, L. R. *et al.* Polyphosphate granule biogenesis is temporally and functionally tied to cell cycle exit during starvation in Pseudomonas aeruginosa. *Proc. Natl. Acad. Sci. U. S. A.* **114,** E2440–E2449 (2017).

38. Bru, S. *et al.* Polyphosphate is involved in cell cycle progression and genomic stability in Saccharomyces cerevisiae. *Mol. Microbiol.* **101,** 367–380 (2016).

39. Kozak, M. Constraints on reinitiation of translation in mammals. *Nucleic Acids Res.* **29,** 5226–5232 (2001).

40. Kozak, M. Pushing the limits of the scanning mechanism for initiation of translation. *Gene* **299,** 1–34 (2002).

41. Matsuda, D. & Dreher, T. W. Close spacing of AUG initiation codons confers dicistronic character on a eukaryotic mRNA. *RNA N. Y. N* **12,** 1338–1349 (2006).

42. Bulankova, P., Riehs-Kearnan, N., Nowack, M. K., Schnittger, A. & Riha, K. Meiotic progression in Arabidopsis is governed by complex regulatory interactions between SMG7, TDM1, and the meiosis I-specific cyclin TAM. *Plant Cell* **22,** 3791–3803 (2010).

43. Riehs, N. *et al.* Arabidopsis SMG7 protein is required for exit from meiosis. *J. Cell Sci.* **121,** 2208–2216 (2008).

44. Tsutsui, H. & Higashiyama, T. pKAMA-ITACHI Vectors for Highly Efficient CRISPR/Cas9-Mediated Gene Knockout in Arabidopsis thaliana. *Plant Cell Physiol.* **58,** 46–56 (2017).

45. Martinez, J., Truffault, V. & Hothorn, M. Structural Determinants for Substrate Binding and Catalysis in Triphosphate Tunnel Metalloenzymes. *J. Biol. Chem.* **290,** 23348–23360 (2015).

46. Meijering, E. *et al.* Design and validation of a tool for neurite tracing and analysis in fluorescence microscopy images. *Cytom. Part J. Int. Soc. Anal. Cytol.* **58,** 167–176 (2004).

47. Schindelin, J. *et al.* Fiji: an open-source platform for biological-image analysis. *Nat. Methods* **9,** 676–682 (2012).

48. Dilba, G., Bretz, F., Guiard, V. & Hothorn, L. A. Simultaneous confidence intervals for ratios with applications to the comparison of several treatments with a control. *Methods Inf. Med.* **43,** 465–469 (2004).

49. Karimi, M., De Meyer, B. & Hilson, P. Modular cloning in plant cells. *Trends Plant Sci.* **10,** 103–105 (2005).

50. Gibson, D. G. *et al.* Enzymatic assembly of DNA molecules up to several hundred kilobases. *Nat. Methods* **6,** 343–345 (2009).

51. Clough, S. J. & Bent, A. F. Floral dip: a simplified method for Agrobacterium-mediated transformation of Arabidopsis thaliana. *Plant J. Cell Mol. Biol.* **16,** 735–743 (1998).

52. Chevallet, M., Luche, S. & Rabilloud, T. Silver staining of proteins in polyacrylamide gels. *Nat. Protoc.* **1,** 1852–1858 (2006).

53. Chomczynski, P. & Sacchi, N. Single-step method of RNA isolation by acid guanidinium thiocyanate-phenol-chloroform extraction. *Anal. Biochem.* **162,** 156–159 (1987).

54. Kurihara, D., Mizuta, Y., Sato, Y. & Higashiyama, T. ClearSee: a rapid optical clearing reagent for whole-plant fluorescence imaging. *Development* **142,** 4168–4179 (2015).

55. Hacham, Y. *et al.* Brassinosteroid perception in the epidermis controls root meristem size. *Development* **138,** 839–848 (2011).

56. Faye, M. D., Graber, T. E. & Holcik, M. Assessment of selective mRNA translation in mammalian cells by polysome profiling. *J. Vis. Exp. JoVE* e52295 (2014). doi:10.3791/52295

**Supplementary Information** is available in the online version of the paper (Extended Data Fig. 1-6, Extended Data Tables 1 and 2, and Supplementary Information).

**Acknowledgments** We thank J.M. Perez-Perez for sending us the CYCB1;1-GFP line, A. Wachter for *lba1* and *upf3-1* seeds, and R. Ulm, A. Wachter and N. Geldner for critical reading of the manuscript. This project was supported by ERC starting grant from the European Research Council under the European Union's Seventh Framework Programme (FP/2007-2013) / ERC Grant Agreement n. 310856, the Max Planck Society, the European Molecular Biology Organisation (EMBO) Young Investigator Programme (to M.H.), and the Howard Hughes Medical Institute (International Research Scholar Award; to M.H.).

**Author Contributions** L. L-O. and M. H. designed the study, L. L-O. performed the majority of the experiments and analyzed data. J. W. and A. P. characterized *ttm3* insertion lines, the *ttm3-2* embryo phenotype, performed localization experiments and produced the TTM3 antibody. J. D. and L. L-O designed and performed the polysome profile assays. J. M. together with L. L-O. purified the AtCDC26 protein and antibody. S. L. quantified CYCB1;1

levels, Y. J. generated transgenic reporter lines, L. A. H. performed statistical analyses, L. L-O., J. W., S. L., L. A. H. and M. H. analyzed data, and Y. P. and M. H. supervised the study. L. L-O. and M. H. drafted the manuscript and all authors discussed the results, edited and approved the final versions of the manuscript.

**Author Information** The authors declare no competing financial interests. Correspondence and requests for materials should be addressed to M.H. (michael.hothorn@unige.ch).

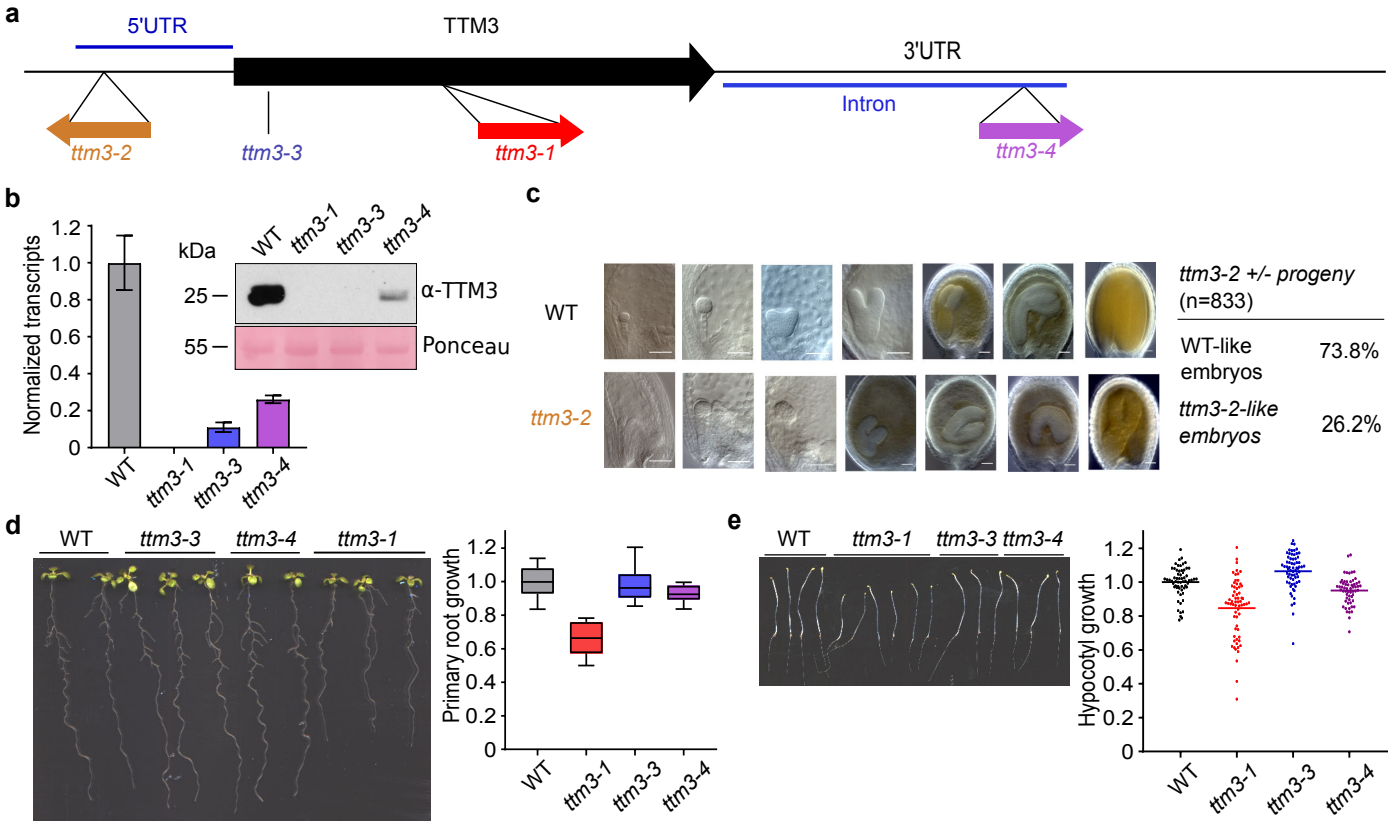
a
5'UTR
TTM3
3'UTR
Intron
ttm3-2
ttm3-3
ttm3-1
ttm3-4
b
Normalized transcripts
kDa
WT
ttm3-1
ttm3-3
ttm3-4
25
55
α-TTM3
Ponceau
c
WT
ttm3-2
ttm3-2 +/- progeny
(n=833)
WT-like embryos
73.8%
ttm3-2-like embryos
26.2%
d
WT
ttm3-3
ttm3-4
ttm3-1
Primary root growth
e
WT
ttm3-1
ttm3-3
ttm3-4
Hypocotyl growth

FIG 1

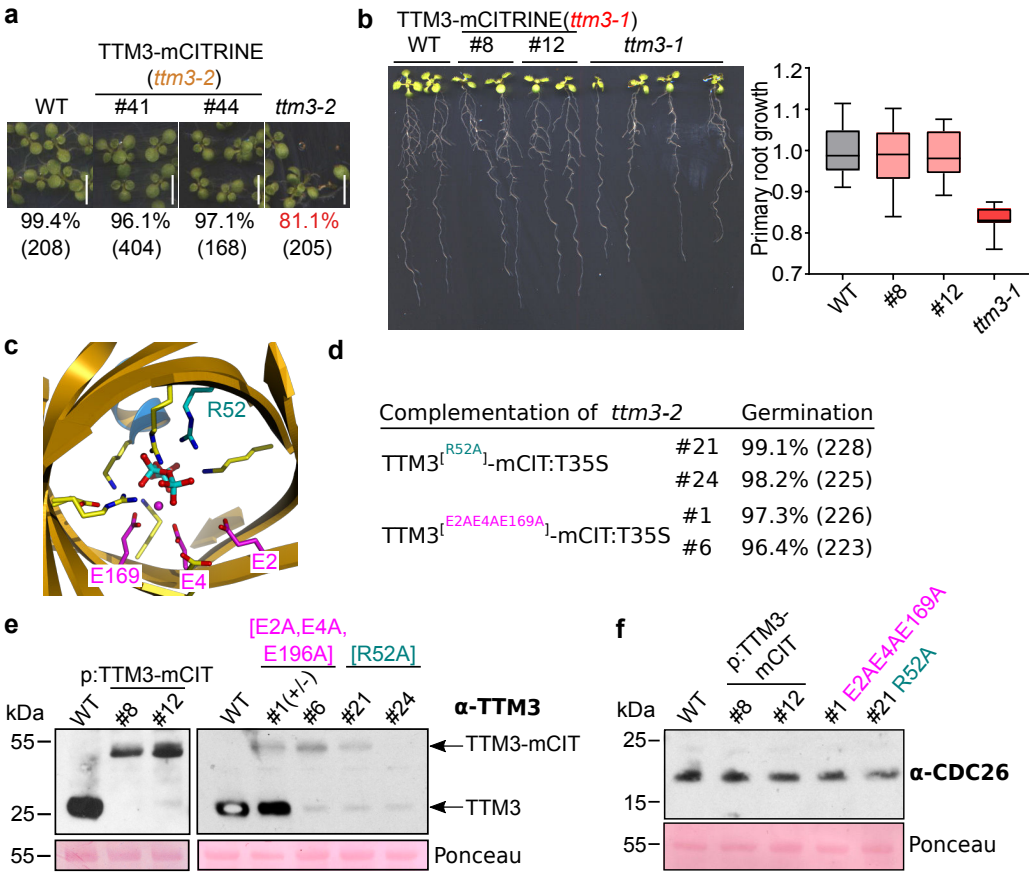
a
TTM3-mCITRINE
(ttm3-2)
WT
#41
#44
ttm3-2
99.4%
(208)
96.1%
(404)
97.1%
(168)
81.1%
(205)
b
TTM3-mCITRINE(ttm3-1)
WT
#8
#12
ttm3-1
Primary root growth
1.2
1.1
1.0
0.9
0.8
0.7
WT
#8
#12
ttm3-1
c
R52
E169
E4
E2
d
Complementation of ttm3-2
Germination
TTM3[R52A]-mCIT:T35S
#21
99.1% (228)
#24
98.2% (225)
TTM3[E2AE4AE169A]-mCIT:T35S
#1
97.3% (226)
#6
96.4% (223)
e
p:TTM3-mCIT
[E2A,E4A,
E196A]
[R52A]
kDa
WT
#8
#12
WT
#1(+/-)
#6
#21
#24
α-TTM3
55
25
55
TTM3-mCIT
TTM3
Ponceau
f
p:TTM3-mCIT
#1 E2AE4AE169A
#21 R52A
kDa
WT
#8
#12
25
15
55
α-CDC26
Ponceau

FIG 2

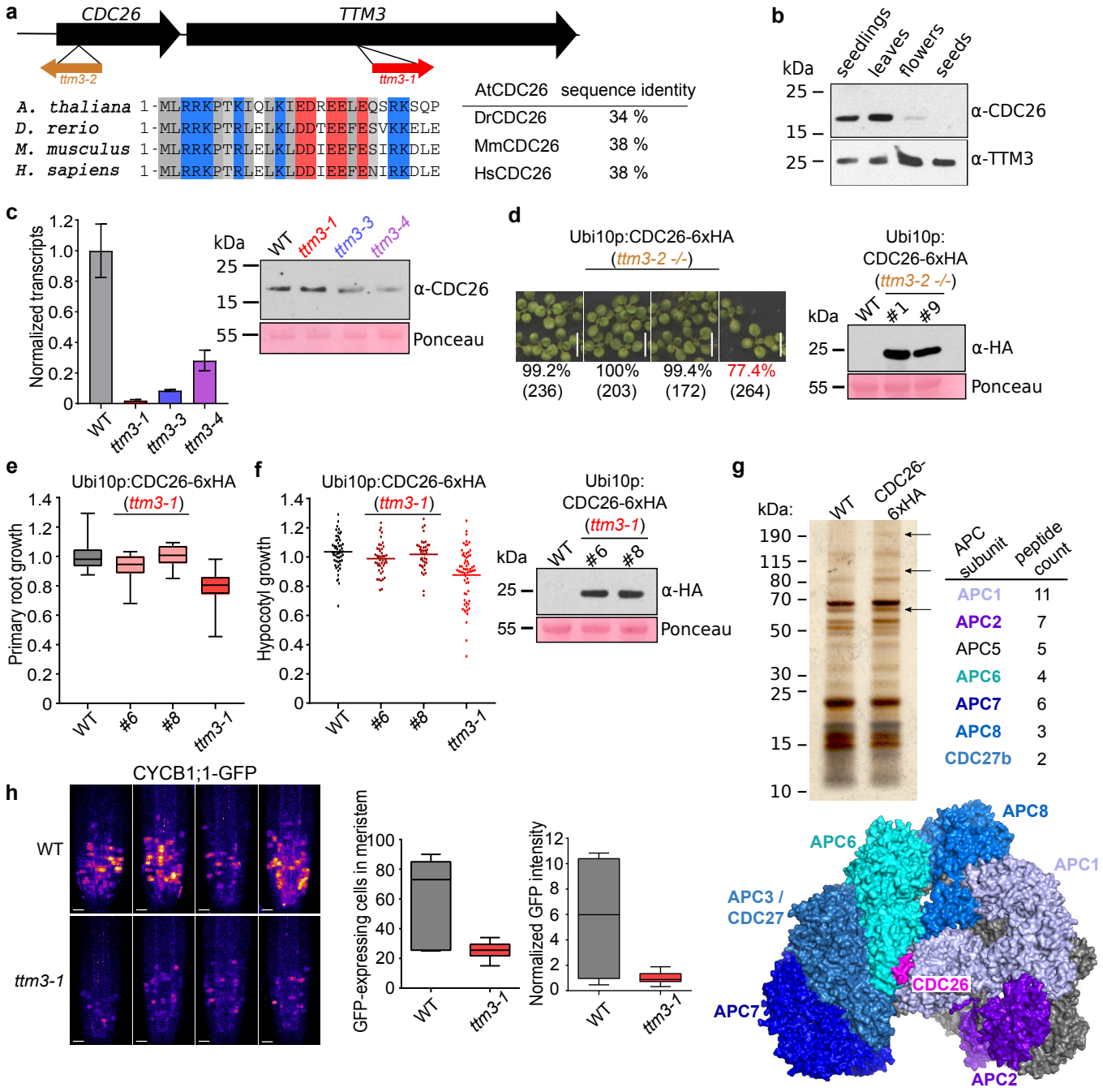
a
CDC26
TTM3
ttm3-2
ttm3-1
A. thaliana 1-MLRRKPTKIQLKIEDREELEQSRKSQP
D. rerio 1-MLRRKPTRLELKLDDTEEFESVKKELE
M. musculus 1-MLRRKPTRLELKLDDIEEFESIRKDLE
H. sapiens 1-MLRRKPTRLELKLDDIEEFENIRKDLE
AtCDC26 sequence identity
DrCDC26 34 %
MmCDC26 38 %
HsCDC26 38 %
b
kDa
seedlings
leaves
flowers
seeds
25
15
25
α-CDC26
α-TTM3
c
Normalized transcripts
WT
ttm3-1
ttm3-3
ttm3-4
kDa
25
15
55
α-CDC26
Ponceau
d
Ubi10p:CDC26-6xHA
(ttm3-2 -/-)
99.2%
(236)
100%
(203)
99.4%
(172)
77.4%
(264)
Ubi10p:
CDC26-6xHA
(ttm3-2 -/-)
kDa
WT
#1
#9
25
55
α-HA
Ponceau
e
Ubi10p:CDC26-6xHA
(ttm3-1)
Primary root growth
WT
#6
#8
ttm3-1
f
Ubi10p:CDC26-6xHA
(ttm3-1)
Hypocotyl growth
WT
#6
#8
ttm3-1
Ubi10p:
CDC26-6xHA
(ttm3-1)
kDa
WT
#6
#8
25
55
α-HA
Ponceau
g
kDa:
WT
CDC26-6xHA
190
115
80
70
50
30
25
15
10
APC subunit
peptide count
APC1 11
APC2 7
APC5 5
APC6 4
APC7 6
APC8 3
CDC27b 2
APC8
APC6
APC1
APC3 / CDC27
CDC26
APC7
APC2
h
CYCB1;1-GFP
WT
ttm3-1
GFP-expressing cells in meristem
WT
ttm3-1
Normalized GFP intensity
WT
ttm3-1

FIG 3

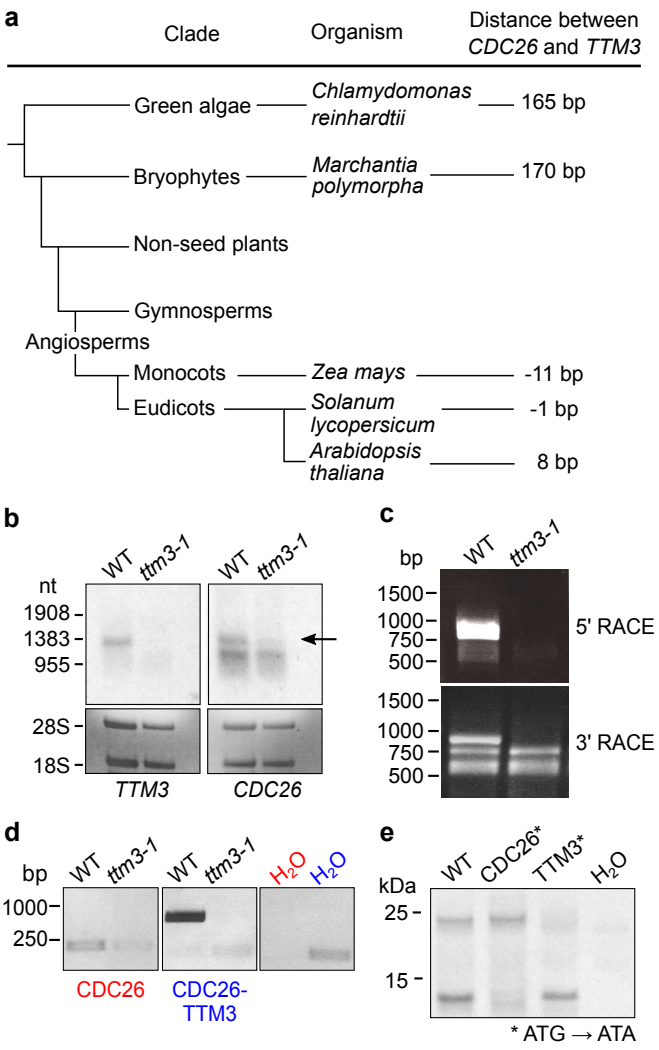
a
Clade
Organism
Distance between CDC26 and TTM3
Green algae
Chlamydomonas reinhardtii
165 bp
Bryophytes
Marchantia polymorpha
170 bp
Non-seed plants
Gymnosperms
Angiosperms
Monocots
Zea mays
-11 bp
Eudicots
Solanum lycopersicum
-1 bp
Arabidopsis thaliana
8 bp
b
WT
ttm3-1
WT
ttm3-1
nt
1908
1383
955
28S
18S
TTM3
CDC26
c
bp
WT
ttm3-1
1500
1000
750
500
5' RACE
1500
1000
750
500
3' RACE
d
bp
WT
ttm3-1
WT
ttm3-1
H2O
H2O
1000
250
CDC26
CDC26-TTM3
e
WT
CDC26*
TTM3*
H2O
kDa
25
15
* ATG → ATA

FIG 4

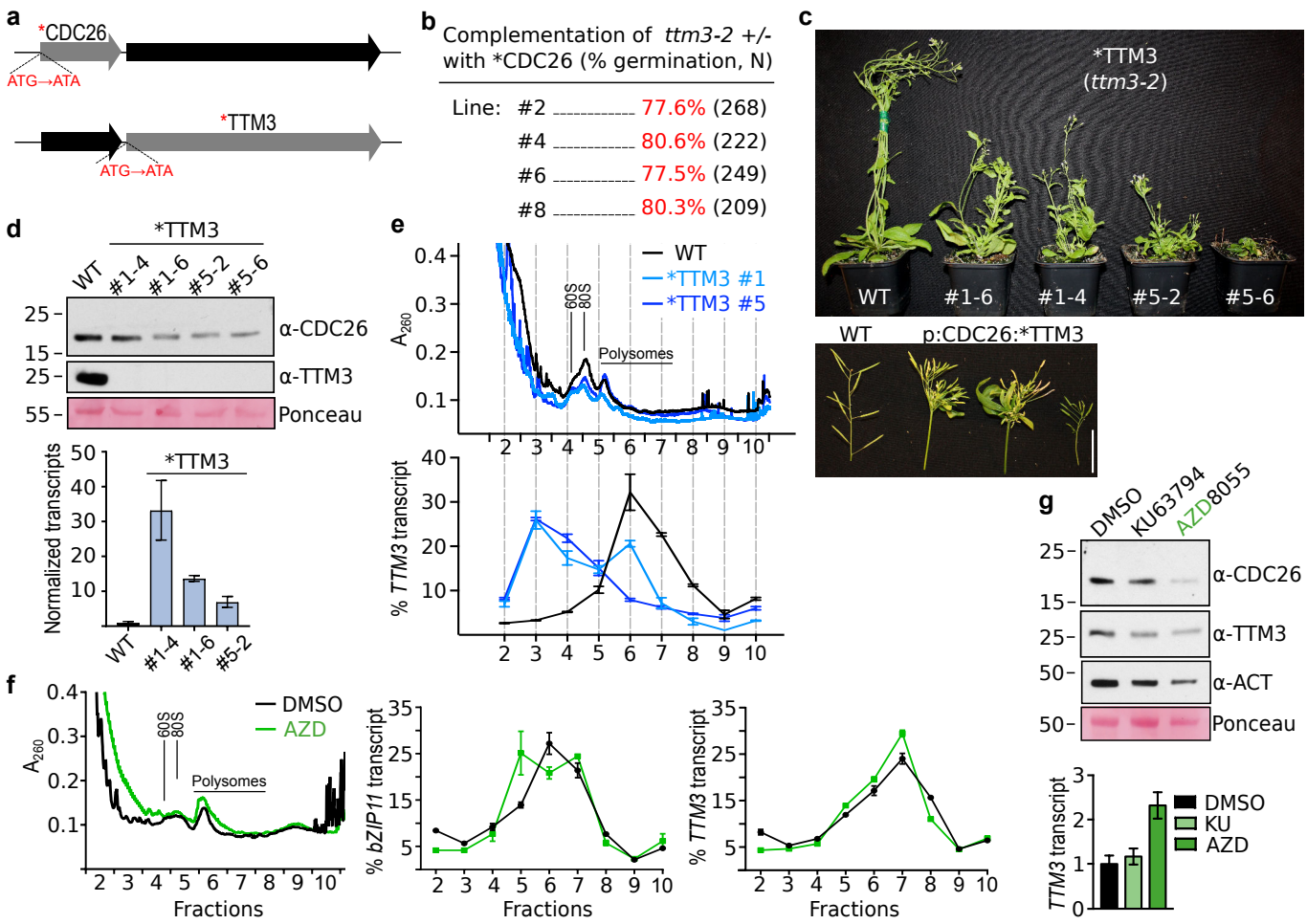
a
*CDC26
ATG→ATA
*TTM3
ATG→ATA
b
Complementation of ttm3-2 +/- with *CDC26 (% germination, N)
Line: #2 77.6% (268)
#4 80.6% (222)
#6 77.5% (249)
#8 80.3% (209)
c
*TTM3 (ttm3-2)
WT
#1-6
#1-4
#5-2
#5-6
WT
p:CDC26:*TTM3
d
*TTM3
WT
#1-4
#1-6
#5-2
#5-6
α-CDC26
α-TTM3
Ponceau
Normalized transcripts
e
WT
*TTM3 #1
*TTM3 #5
60S
80S
Polysomes
% TTM3 transcript
f
DMSO
AZD
Polysomes
% bZIP11 transcript
% TTM3 transcript
Fractions
g
DMSO
KU63794
AZD8055
α-CDC26
α-TTM3
α-ACT
Ponceau
TTM3 transcript
DMSO
KU
AZD

FIG 5

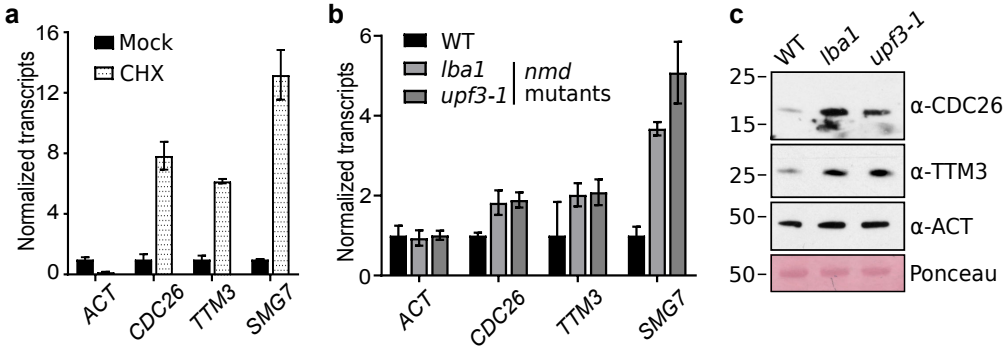
a
Mock
CHX
Normalized transcripts
16
12
8
4
0
ACT
CDC26
TTM3
SMG7
b
WT
lba1
upf3-1
nmd
mutants
Normalized transcripts
6
4
2
0
ACT
CDC26
TTM3
SMG7
c
WT
lba1
upf3-1
25
15
25
50
50
α-CDC26
α-TTM3
α-ACT
Ponceau

FIG 6

**a**

TTM3

```
C. reinhardtii     1- MEVEIKIRLPDRAAYEQVAAALAAAPGGKGRLDSHAQGYRMVLVTPTSRCARPHQANYFFDGPNQELNSRRVVLRVRTYDVD---- -82
M. polymorpha      1- MEVEVKLKLPGREAHEKVASSLKAF----------------------HEVTHMQENVFFDGANKELSSKRAVLRLRFYNGD---- -59
Z. mays            1- MEVEIKLRLPDAAAHRRLSAFLAP----------------------RLRRTHAQRNLFFDDAARTLGAATAALRVRLYDGPDD-- -61
S. lycopersicum    1- MEVEVKLRLPDSSAHQKVLSLFSS----------------------HHKKTHHQRNTFFDGAAGELSSRRAVLRLRFYENSE--- -60
A. thaliana        1- MEVEVKLRLLTAAAHLRLTTLLTP----------------------YHLKTLHQRNTFFDTPKNDLSLRRAVLRLRFLQNAAVSA -63

C. reinhardtii    83- -----KKATVTLKGKQILENGIGRASEVEAEVPPAAAAAYLTQPSRML-AEVPIVKDAAEKFGVG----SLVALGGFQNQRDVYEW -158
M. polymorpha     60- -----GKCVVTFKGNAVIVDGISRGEELEEDIDVSLGRACVAEPWRLATTTCKLLNKVVADFAC----EDFVCLGGFRNVRTVFNW -136
Z. mays           62- --RGPSRAVLALKRRPRIEAGVSRVEEIEEPLEPALAVACADDPARLGGLDSPIIRLVAAEYGVGGDAAPFLCLGGFGNTRAVYEY -145
S. lycopersicum   61- ----KVKCMVCLKAKAVIIDGVSRVEEDEEELDPKIGYECVSNPRKLMEVDSRVLKRAREEFHVG-E-EGFIGLGGFKNVRNVFEW -140
A. thaliana       64- ASPSPPRCIVSLKAKPTLANGISRVEEDEEEIEYWIGKECVESPAKLSDIGSRVLKRVKEEYGFN-DFLGFVCLGGFENVRNVYEW -148

C. reinhardtii   159- E------GHTLELDETKFEHGTLYEIEVETEQPEVLRDRLEHWLSGMGVSYSYSQTSKFANFINKTLL- -220
M. polymorpha    137- E------GLKIELDETQYDFGTTYEVECESTDPERVREVLGDFLKSKGIEFTYSTKSKFAVFRSGKIE- -198
Z. mays          146- ELEDGGGGLVLELDETRFDFGTRYELECETAEPDRVKEVLERLLTVAGVPYEYCRNSKFACFMTGKLLP -214
S. lycopersicum  141- C------GVELEVDETMYDFGTFYEIECESLEPEKVKAMIEAFLKDNDIDYSYSEVSKFATFRAGKLP- -202
A. thaliana      149- R------GVKLEVDETKYDFGNCYEIECETEEPERVKTMIEEFLTEEKIEFSNSDMTKFAVFRSGKLP- -210
```

| AtTTM3 protein | Identity |
|---|---|
| CrTTM3 | 39 % |
| MpTTM3 | 47 % |
| ZmTTM3 | 45 % |
| SlTTM3 | 59 % |

**b**

CDS

deleted in *ttm3-3*

```
TTM3      1 - ATGGAAGTCGAAGTCAAGCTCCGTCTCCTAACCGCCGCTGCTCATCTCCGTCTCACCACTCTCCTCACTCC(...)TGA - 633
ttm3-3    1 - ATGGAAGTCGAAGTCAAGCTCC                TGCTCATCTCCGTCTCACCACTCTCCTCACTCC(...)TGA - 617
```

Protein

```
TTM3      1 - MEVEVKLRLLTAAAHLRLTTLLTPYHLKTLHQRNTFFDTPKNDLSLRRAVLRLRFLQNAAVSAASPSPPRCIVSLA(...)KLP - 210
ttm3-3    1 - MEVEVKLLLISVSPLSSLHTTSKPFTNATPSSTHPKTTSLSAAPSSVSASFKTPPFPRLLLLRRVVSSLLKRSQL          - 75
```

FIG S1

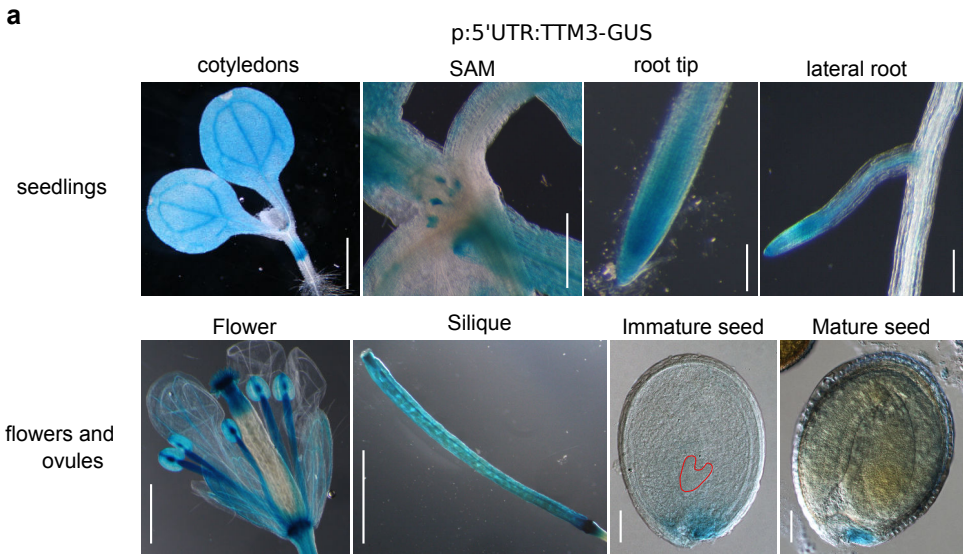
a
p:5'UTR:TTM3-GUS
cotyledons
SAM
root tip
lateral root
seedlings
Flower
Silique
Immature seed
Mature seed
flowers and ovules

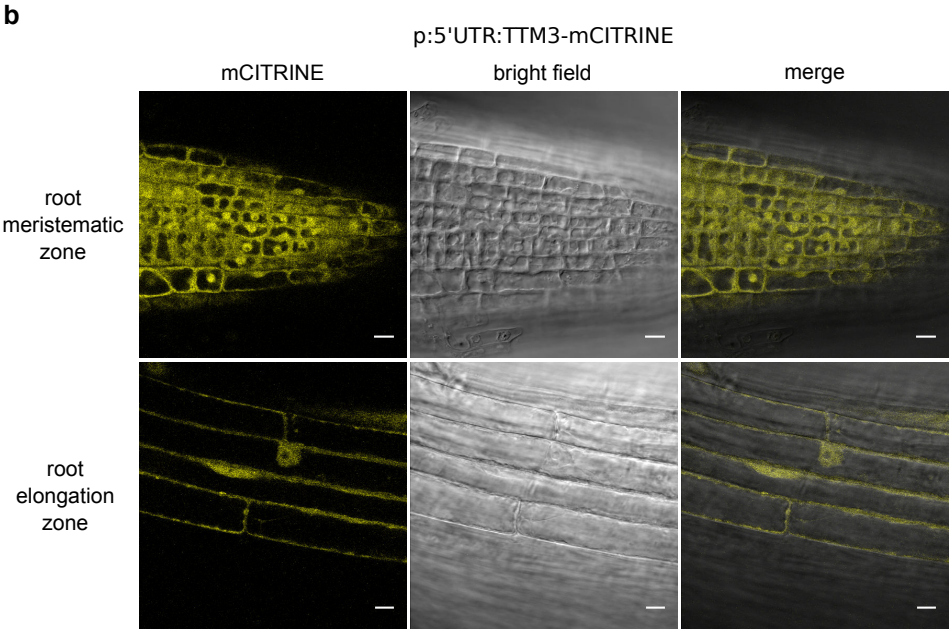
b
p:5'UTR:TTM3-mCITRINE
mCITRINE
bright field
merge
root meristematic zone
root elongation zone

FIG S2

**a**

> ***C. reinhardtii***
CRgenome|CrChr16[1870194-1870688]

-492
ATGCTGCCGCGCAAGCCTACTCGCATAGATCTCAAGCCAGCGGACAAGGAAGAGGTCAGAACTCTGCTCTGGGACCTGGCTGTTCGCGCGTCGATTCCATTATTTGGG
GTTCGCTATACGACAGCCATTTCTCCTTCCCTTGCTCCTACAGTACGAGAACCTCAAAGCTTTACAGCTGGAGCGCAAAGCGGCCCTGGAGCACGCTTCGGACGCGTT
CTTGCCCGATCCTCTCCAGGTCCGCCGCGGCGGGGGTTGGGACCCAACGATTGCAGGGGTGCGGGTCGAGGGATGGCGCATAGGTTATCTAGAACAGTTGCAGCGGTC
TGAGAGGCCCTGTGCGGGGCGGCCGGGCACCACACACACCCGCCTCTTCCCCTACCCCATCTGCGCGCGACTCTAAACCACCCCTCATACCTTGACCCCGCCTGCCGG
TGTGCCGCAGGTGGAGAAGCGCTCCACGGCGGCGCGGATAGGCCTGCGGAAGTGAGGCCCATG
+1

> ***M. polymorpha***
scaffold00152[209114-209505]

-389
ATGTTGAAGAGGAAGCCGACGAGGCTCGAGTTCAAGGAGGCCGATGACAAGGAGGATCTAGAGCAAGCACGGAAGAGCGCATCTGCTGCCGCCGCTGCTGCTGCTGCG
GCTTCGTCTGCAGGTGCTGCTGCCGTTGGTGGCTCTGCTTCTGCTACCCCGCAAGTCATCGAATTTCGCCCTAAACTTTCTGTCGCTCAACGAATAGGATTCAACAAG
TAGTTGTGCTGCAGCGTGTGAATTTTGTGGGTGCGGGCCCGCACGCCGTTGCGCAAGGCGTGGCCGAGTGGTGGTGTGGTGGTACTTTCCCTTGGTGTTTGTACATTG
GACTGGGTTAATAAATTTTGCTCGGACTGCAAGAGAGTGGCGGTTTGTTCTCTTCGGTTCTCGGAATG
+1

> ***Z. mays***
NW_007617763.1:174002602-174002886 Zea mays cultivar B73 chromosome 7 genomic scaffold, B73 RefGen_v3 7

-274
ATGCTGCGCCGCAACCCAACCCatgctgcgccgcaaGCATCGAGCTCACCTCCTCCGACCGCGACGAGCTCGAAGACCACCTCCGCGCCGCCGCGGCAGCCACCACCA
CCAAGGATCCTTCCGGTTACACCACTCCGTCTCCAGTCCTTGGCCCGCAGACCTCCAATCCCCTGCTCCAATTCCTCCACCCGAAGCCCGGCGCCGTGCCATCCAAGT
CCCAACGCATCGGCATCGGCCTCTCCACCCCGCCGGCTCCGGCCCCGAACCCGCGACCACCCCATCCACCCCATGGAGGTTGA
+1

> ***S. lycopersicum***
SL3.0ch07[2203432-2203209]

-221
ATGCTGAGAAGAAAGCCCAGCAAAATCGAAGTAAAAATCGAAGACAAAGAAGAACTCGAAGAAGCTCGCAAACGCGCCGCCCTCATCGCCGCCTCTTCCTCCACCAGT
ACCGCCGCCGGTACCGGCGGAGCTGCCACAGCCGGTGTCTCCTCTCTCCTCCAACACTTCGACCGATCAACAGTCGATCCTTCCTCCAAAAACAACCGCATCGGCCTC
AATTAATG
+1

> ***A. thaliana***
Chr2[4802793-4803002]

-206
ATGTTGAGAAGAAAACCAACAAAAATCCAACTCAAAATCGAAGACCGTGAAGAGCTTGAACAATCCCGCAAATCTCAACCATCCACCACCACAACCACCGCACCATCT
TCCTCCTCCGCCGCCTCCTCTCTCCACCACCTCATAGACCCAAAACACAAAAACCCTTCCTCCAAATCCGACCGAATCGGTCTCTCTTAAAACACTCCATG
+1

**b**

| Organism | cDNA clone (Sequence ID) | Length |
|---|---|---|
| *C. reinhardtii* | XM_001697825.1 | 2039 bp |
| *Z. mays* | BT037955.1 | 1237 bp |
| *S. lycopersicum* | AK321570.1 | 1134 bp |
| *A. thaliana* | AK316974.1 | 949 bp |

**c**

ANAPC_CDC26 motif

```
C. reinhardtii   1- [redacted]VRASIP----------LFGVRYTTAISPSLAPTVREPQSFTAGA -61
M. polymorpha    1- [redacted]AAAAAAAAAASSAGAAAVGGSASATPQVIEFRPK---------- -61
Z. mays          1- [redacted]AATTTKDPSGYTTPSPVLGPQTSNPLLQFLHPKPGA-------- -63
S. lycopersicum  1- [redacted]LIAASSSTSTAAGTGG-AATAGVSSLLQHFDRSTVD-------- -62
A. thaliana      1- [redacted]STTTTT--------AP-SSSSAASSLHHLIDPKHKN-------- -54

C. reinhardtii   62- QSGPGARFGRVLAR--------SSPGPPRRGLGPNDCRGAGRGMAHRLSRTVAAV -108
M. polymorpha    62- -LSVAQRIGFNK---------------------------------------- - 72
Z. mays          64- VPSKSQRIGIGLSTPPAPAPNPRPPHPPHGG------------------------ - 94
S. lycopersicum  63- PSSKNNRIGLN---------------------------------------------- - 73
A. thaliana      55- PSSKSDRIGLS---------------------------------------------- - 65
```

| AtCDC26 protein | Identity |
|---|---|
| CrCDC26 | 25 % |
| MpCDC26 | 39 % |
| ZmCDC26 | 40 % |
| SlCDC26 | 46 % |

FIG S3

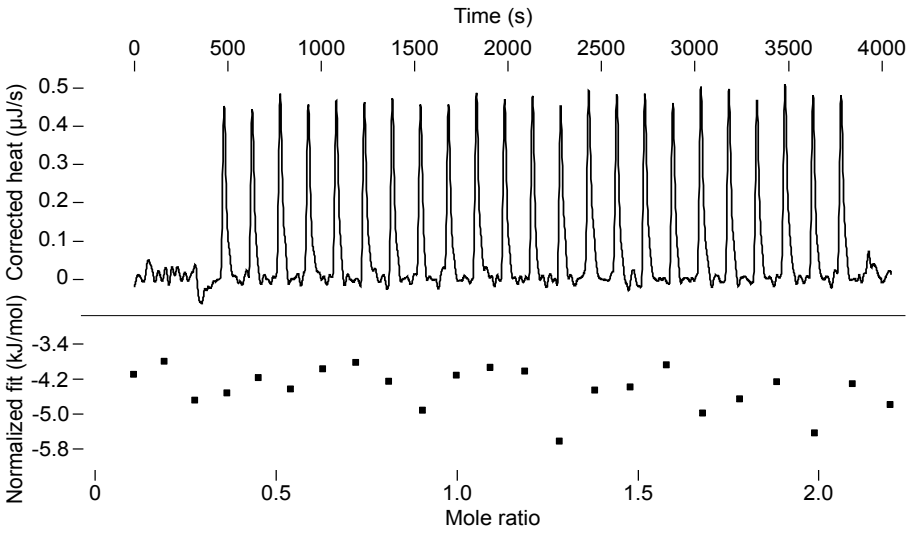
Time (s)
0
500
1000
1500
2000
2500
3000
3500
4000
Corrected heat (µJ/s)
0.5
0.4
0.3
0.2
0.1
0
Normalized fit (kJ/mol)
-3.4
-4.2
-5.0
-5.8
0
0.5
1.0
1.5
2.0
Mole ratio

FIG S4

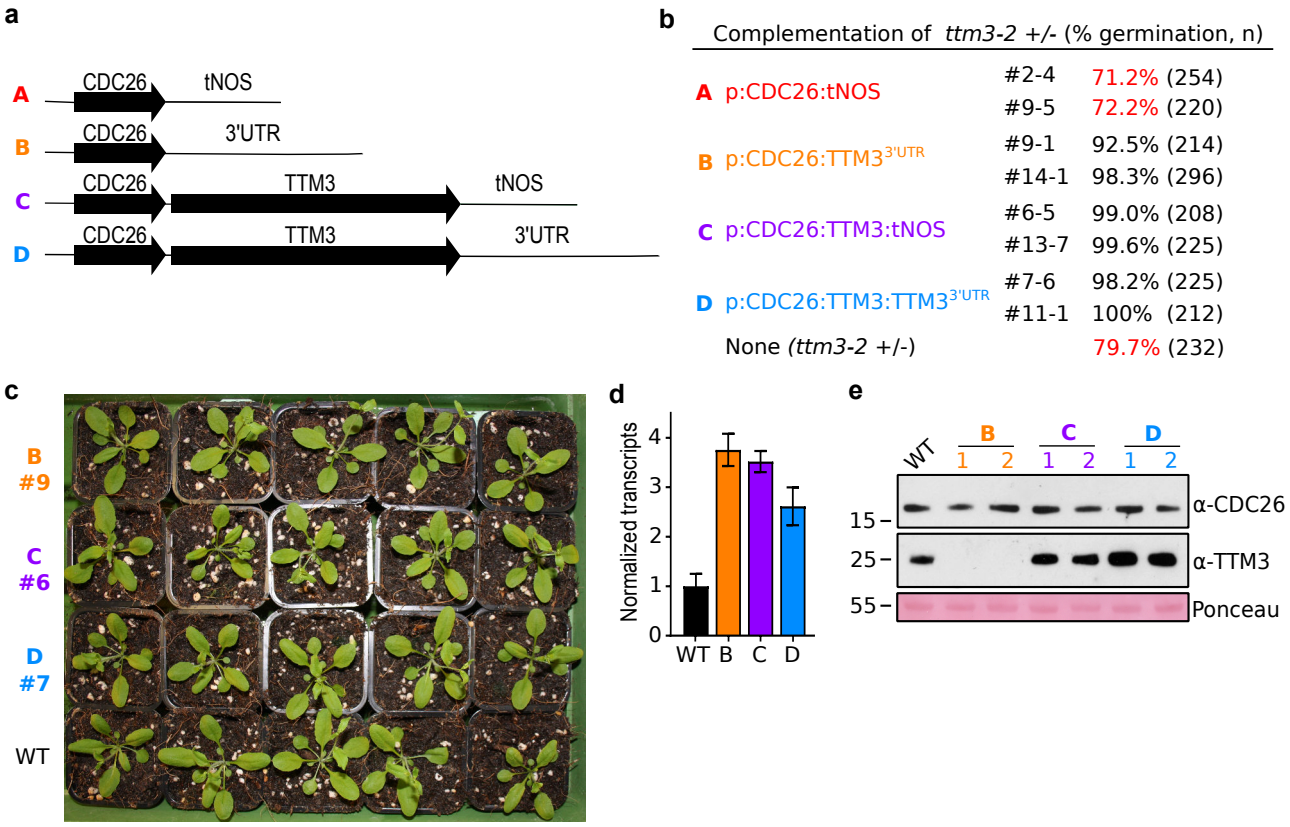
a
A
CDC26
tNOS
B
CDC26
3'UTR
C
CDC26
TTM3
tNOS
D
CDC26
TTM3
3'UTR
b
Complementation of ttm3-2 +/- (% germination, n)
A p:CDC26:tNOS
#2-4 71.2% (254)
#9-5 72.2% (220)
B p:CDC26:TTM3 3'UTR
#9-1 92.5% (214)
#14-1 98.3% (296)
C p:CDC26:TTM3:tNOS
#6-5 99.0% (208)
#13-7 99.6% (225)
D p:CDC26:TTM3:TTM3 3'UTR
#7-6 98.2% (225)
#11-1 100% (212)
None (ttm3-2 +/-)
79.7% (232)
c
B #9
C #6
D #7
WT
d
Normalized transcripts
0
1
2
3
4
WT B C D
e
WT
B
C
D
1 2 1 2 1 2
15
25
55
α-CDC26
α-TTM3
Ponceau

FIG S5

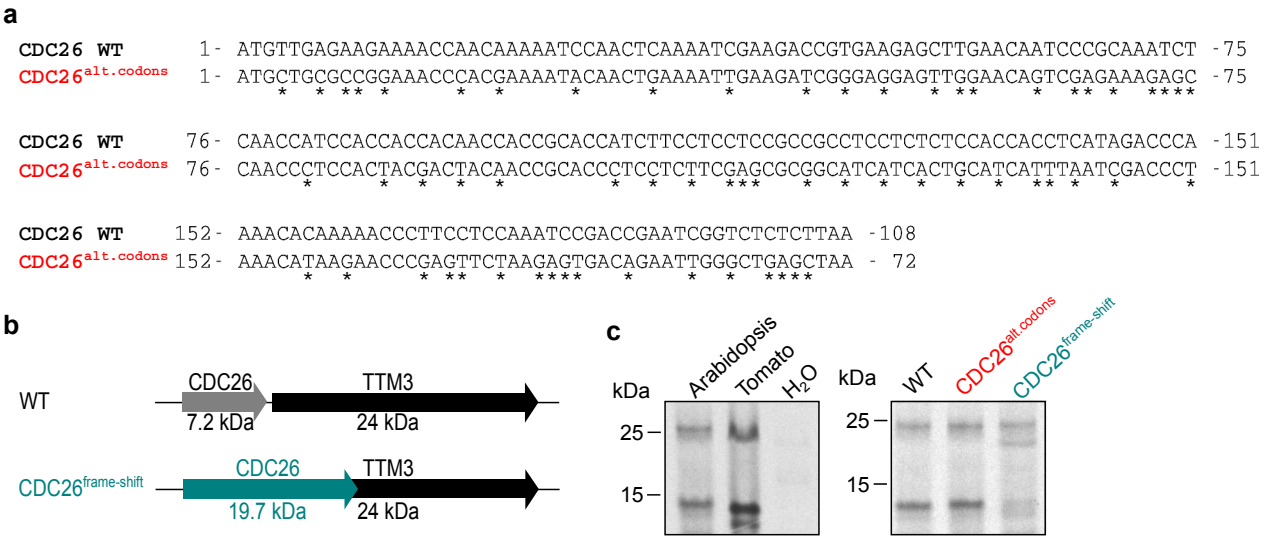
a
CDC26 WT 1- ATGTTGAGAAGAAAACCAACAAAAATCCAACTCAAAATCGAAGACCGTGAAGAGCTTGAACAATCCCGCAAATCT -75
CDC26alt.codons 1- ATGCTGCGCCGGAAACCCACGAAAATACAACTGAAAATTGAAGATCGGGAGGAGTTGGAACAGTCGAGAAAGAGC -75
CDC26 WT 76- CAACCATCCACCACCACAACCACCGCACCATCTTCCTCCTCCGCCGCCTCCTCTCTCCACCACCTCATAGACCCA -151
CDC26alt.codons 76- CAACCCTCCACTACGACTACAACCGCACCCTCCTCTTCGAGCGCGGCATCATCACTGCATCATTTAATCGACCCT -151
CDC26 WT 152- AAACACAAAAACCCTTCCTCCAAATCCGACCGAATCGGTCTCTCTTAA -108
CDC26alt.codons 152- AAACATAAGAACCCGAGTTCTAAGAGTGACAGAATTGGGCTGAGCTAA - 72
b
WT
CDC26
7.2 kDa
TTM3
24 kDa
CDC26frame-shift
CDC26
19.7 kDa
TTM3
24 kDa
c
kDa
Arabidopsis
Tomato
H2O
25
15
kDa
WT
CDC26alt.codons
CDC26frame-shift
25
15

FIG S6